Molecular Therapy
Nucleic Acids
Original Article

An Albumin-Oligonucleotide Assembly for Potential Combinatorial Drug Delivery and Half-Life Extension Applications

Matthias Kuhlmann,[1] Jonas B.R. Hamming,[1] Anders Voldum,[1] Georgia Tsakiridou,[1] Maja T. Larsen,[1] Julie S. Schmøkel,[1] Emil Sohn,[1] Konrad Bienk,[1] David Schaffert,[1] Esben S. Sørensen,[1] Jesper Wengel,[2] Daniel M. Dupont,[1] and Kenneth A. Howard[1]

[1]Interdisciplinary Nanoscience Center (iNANO), Department of Molecular Biology and Genetics, Aarhus University, 8000 Aarhus C, Denmark; [2]Nucleic Acid Center, Department of Physics, Chemistry, and Pharmacy, University of Southern Denmark, Campusvej 55, 5230 Odense M, Denmark

The long blood circulatory property of human serum albumin, due to engagement with the cellular recycling neonatal Fc receptor (FcRn), is an attractive drug half-life extension enabling technology. This work describes a novel site-specific albumin double-stranded (ds) DNA assembly approach, in which the 3′ or 5′ end maleimide-derivatized oligodeoxynucleotides are conjugated to albumin cysteine at position 34 (cys34) and annealed with complementary strands to allow single site-specific protein modification with functionalized ds oligodeoxynucleotides. Electrophoretic gel shift assays demonstrated successful annealing of complementary strands bearing Atto488, 6-carboxyfluorescein (6-FAM), or a factor IXa aptamer to the albumin-oligodeoxynucleotide conjugate. A fluorometric factor IXa activity assay showed retained aptamer inhibitory activity upon assembly with the albumin and completely blocked factor IXa at a concentration of 100 nM for 2 hr. The assembled construct exhibited stability in serum-containing buffer and FcRn engagement that could be increased using an albumin variant engineered for higher FcRn affinity. This work presents a novel albumin-oligodeoxynucleotide assembly technology platform that offers potential combinatorial drug delivery and half-life extension applications.

INTRODUCTION

Site-specific delivery and target engagement are prominent determinants of the therapeutic efficacy of drugs.[1] Molecular medicines, such as RNA-interference-[2,3] and aptamer-based[1,4–7] therapeutics offer unprecedented target specificity; however, susceptibility to nuclease degradation and rapid renal clearance require enabling technologies to realize the clinical potential. Although chemical modifications, such as 2′-sugar (2′-fluoro, 2′-O-methyl, etc.)[6] or locked nucleic acids,[8] have overcome stability issues, alternative blood half-life extension technologies are needed to overcome drawbacks associated with poly(ethylene glycol) (PEG), such as non-degradability and possible immune induction.[9–11] PEG immunogenicity, for example, was recently suggested to be the cause of the serious allergic reactions observed with an aptamer-based anticoagulant system targeting factor IX (REG1) in the RADAR phase 2b clinical trial.[12,13]

Human serum albumin (HSA) is an attractive drug delivery platform due to its long-circulatory half-life of ∼19 days,[14] facilitated by engagement with the cellular recycling neonatal Fc receptor (FcRn).[15,16] This property has been exploited in marketed albumin-binding drugs, such as Levemir and Victoza, that reversibly associate with the endogenous albumin pool.[10,17,18] Albumin is structurally divided into three domains, with domain III (DIII) playing the major role in FcRn binding[19] and domain I (DI) containing a single free thiol at position 34 (cys34). Site-specific covalent conjugation of drugs to endogenous HSA or preconjugation to recombinant human albumin (rHA) at position cys34 is, therefore, an attractive strategy for maintained FcRn engagement.[20] Kratz et al.[21] have exploited site-specific maleimide-based drug conjugation for attachment of doxorubicin to the endogenous HSA pool. A limitation of conjugation to the single free thiol of endogenous HSA or rHA, however, is the inability for loading at a final drug:albumin ratio greater than 1:1.[22] Although conjugation to albumin's multiple surface lysines may overcome this caveat, the absence of site selectivity may compromise FcRn engagement and concomitant albumin pharmacokinetics.

Oligodeoxynucleotides (ODNs) have found wide applications in fundamental research and as potential therapeutics.[23,24] The high specificity of base pairing allows engineering of complex DNA structures in a controlled manner that has fueled the emerging field of DNA nanotechnology.[25,26] We propose site-specific conjugation of ODN with the single thiol of rHA at cys34 (referred to as rHAODN) in conjunction with complementary strand (cODN) annealing for introduction of up to three (different) functionalities using the ODN termini (Figure 1). This versatile strategy allows the potential drug loading of ODN and cODN precursors prior to rHA conjugation and cODN annealing. This system may have the potential to combine

Received 5 March 2017; accepted 4 October 2017;
https://doi.org/10.1016/j.omtn.2017.10.004.

Correspondence: Kenneth A. Howard, Interdisciplinary Nanoscience Center (iNANO), Department of Molecular Biology and Genetics, Aarhus University, DK-8000 Aarhus C, Denmark.
E-mail: kenh@inano.au.dk

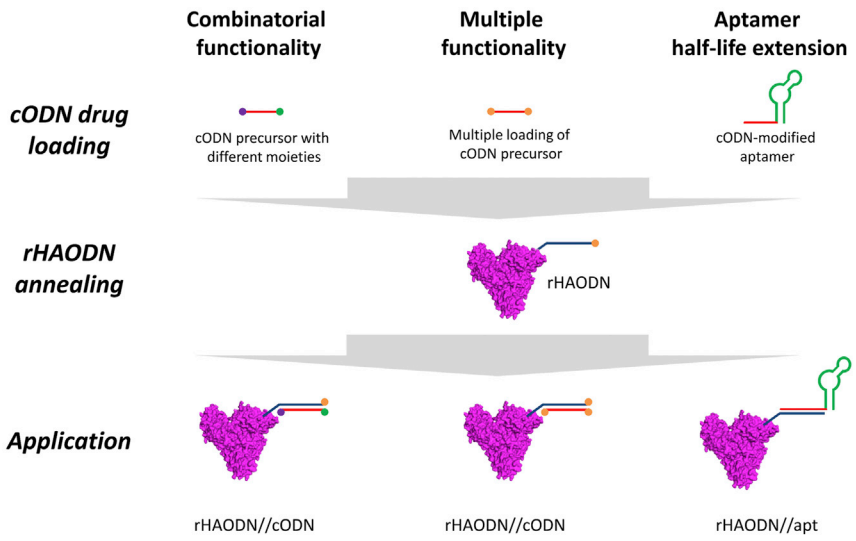

Figure 1. Schematic Representation of Albumin-Oligonucleotide Assembly

cODN precursors can be loaded with drugs (e.g., aptamers) or functional groups before complementary annealing to a rHAODN conjugate for potential combinatorial functions or multiple drug delivery approaches. In addition, an additional functionality can be attached to the free ODN termini.

the target specificity of aptamers with the long circulatory half-life of albumin for next-generation molecular medicines. As proof-of-concept, rHAODN conjugates were annealed with various cODN variants (rHAODN//cODN) to generate constructs that were specifically labeled with or without fluorophores at different positions of the resulting double strand (dsODN) to demonstrate robust assembly independent of the ODN orientation (5′ to 3′ or 3′ to 5′) and functionalization position (ODN or cODN). The rHAODN conjugate was further annealed with a cODN-bearing factor IXa (FIXa)-blocking aptamer, producing a construct (rHAODN//apt) that exhibited retained aptamer activity and FcRn engagement and high stability in serum-containing buffer, prerequisites for potential therapeutic applications.

RESULTS

The ODN sequences and code numbers used in this work are included in Table S1.

Maleimide Functionalization of ODN

Maleimide functionalization ("activation") of ODN 5′ end or 3′ end amines was optimized by varying the pH and reaction time using a commercial succinimidyl 4-(N-maleimidomethyl)cyclohexane-1-carboxylate (SMCC) linker. Urea gel electrophoresis and band intensity quantification (exemplified with ODN1; Figure 2) revealed optimal activation yields after 16–24 hr at a slightly elevated pH (HEPES, pH 8), with an excess of SMCC (SMCC:ODN1 = 50:1). Oligonucleotide activation was similarly efficient for the other ODNs, irrespective of sequence, the position of the amine, and whether or not a fluorophore was attached (exemplified with ODN2, ODN3, and ODN8*; Figure S1). Reverse-phase high-performance liquid chromatography (RP-HPLC) purification (exemplified with ODN4*; Figure S2) verified the optimal activation conditions, and a yield of more than 50% activated ODN was obtained for a 16-hr reaction at pH 8. Subsequent urea-PAGE gel analysis was used to confirm the identity of the purified products (exemplified with ODN1; Figure S3). RP-HPLC-purified SMCC-ODNs were desalted and freeze dried and stock solutions were prepared in nuclease-free water or buffer for further experiments.

rHA Conjugation to SMCC-Activated ODNs

Conjugation of rHA with SMCC-ODN (at a ratio of 1:1) was performed in HEPES buffer (pH 7.0) at room temperature (RT). After 2 hr, SDS gel electrophoresis analysis showed conjugation by both nucleic acid staining (exemplified with ODN3; Figure 3A, upper panel) and rHA staining (Figure 3A, lower panel). Detection of both residual free rHA and the rHAODN3 conjugate by MALDI-ToF analysis confirmed the conjugation (Figure 3B). Two different batches of ODN3 were activated with SMCC (in Figure 3 denoted as SMCC-ODN3 *a* and SMCC-ODN3 *b*) and conjugated to rHA in order to show batch-to-batch reproducibility. In contrast, non-activated ODN3 did not react with rHA (Figure 3A, lane 4). Conjugation was repeated with an SMCC-activated 6-carboxyfluorescein (6-FAM)-labeled ODN (Table S1, ODN4*) to demonstrate the possibility of exploiting the available 3′ end of the ODN for functionality introduction, e.g., a fluorescent probe, to the albumin-oligo assembly. Coomassie protein staining and fluorophore detection of 6-FAM-labeled rHAODN4* confirmed the conjugation (Figure S4). Furthermore, it was shown that a 3′-SMCC-activated ODN (ODN2; Figure S5) reacts similarly efficiently with rHA compared to 5′-SMCC-activated ODNs. Ellman's assay analysis of the rHA stock detected ~54% free thiols and, therefore, even with complete ODN conjugation to all available cys34 thiols in the preparation, free rHA is expected to be present after the reaction. Protein band intensity quantification of the rHA:SMCC-ODN4* reaction (Figure S4) revealed 55%–65% conjugation that correlated with Ellman's determination, showing high reactivity of the available cys34 toward activated ODNs.

rHAODN conjugates were purified from residual rHA using ion-exchange chromatography (IEX). The high negative charge introduced by ODN conjugation shifted the retention time to 48.6 min for the conjugate compared to 30 min for pure rHA (Figure S6). The collected conjugate fractions were desalted, freeze dried, and dissolved in nuclease-free water. Direct quantification of the rHAODN concentration using UV spectroscopy could not be performed because both ODN and rHA absorption spectra overlap (not shown). A Bradford assay was, therefore, used to determine the rHAODN conjugate concentration calibrated with pure rHA. A yield of only

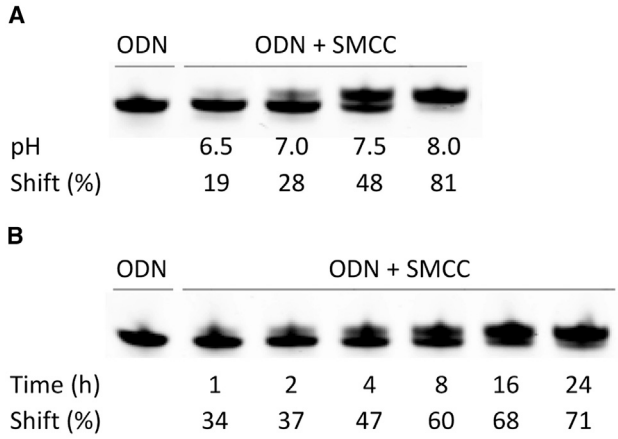

Figure 2. Activation of ODN with SMCC

(A) Urea gels were stained using SYBR gold and band intensity analysis used to determine the activation efficiency. ODN1 (lower band) and SMCC-ODN1 (upper band, activated) were observed. Increase of pH from 6.5 to 8.0 increased the yield from 19% to 81% of activated ODN1 at 16 hr at room temperature. (B) Reactions at pH 8.0 show that SMCC activation increased, with a prolonged reaction time from 1 hr to 24 hr.

10% for the purified conjugate was obtained; the purification process, therefore, requires further investigation and optimization.

Annealing of rHAODN with cODN

To evaluate annealing specificity, Atto488-labeled complementary cODN5* was assembled with either the rHAODN3 or the rHAODN6 conjugate in 0.1 M HEPES buffer (pH 7.0) overnight at RT. Incubation of the conjugate rHAODN6 with cODN5*, which both have the same oligonucleotide sequence, showed no indication of non-specific annealing (Figure 4, lane 1, 3, and 5; negative control [nc]). For assembly of the rHAODN3//cODN5* construct containing a complementary ODN:cODN set, different rHAODN3:cODN5* ratios were used (1:0.5 [Figure 4, lane 2], 1:1 [Figure 4, lane 4], and 1:2 [Figure 4, lane 6]) and the band intensities of rHAODN3 and the annealed construct (rHAODN3//cODN5*) were analyzed (Figure 4, protein staining). Relative to the experiment with a two-fold excess of cODN5* (rHAODN3:cODN5* = 1:2, [Figure 4, lane 6]), a product yield of 60%–65% (1:0.5) and 90%–95% (1:1) was observed. Hence, further excess of cODN would not dramatically increase product yield.

To show that the rHAODN3 conjugate can also be annealed to a cODN strand without a fluorophore attached, we verified product formation using cODN7, i.e., cODN5* without the fluorophore (rHAODN3//cODN7; Figure S7A). The results of annealing rHAODN3 with cODN5* or ODN8* were included as a positive and negative control, respectively. Finally, we wanted to demonstrate that the annealing was independent of the fluorophore being attached to the rHA-conjugated ODN strand ("direct labeling") or the cODN strand annealed to rHAODN ("indirect labeling"). To verify the direct labeling, 3′-Atto488-labeled ODN8* was conjugated to rHA (Figure S7B, Conj.*) and annealed with non-labeled cODN7 to produce the rHAODN8*//cODN7 construct.

Annealing of rHAODN with an FIXa-Blocking Aptamer

To allow conjugation of the aptamer with rHAODN3, the aptamer was extended with the complementary DNA sequence to ODN3 in the 3′ end during synthesis (cODN-aptamer). The final design of the rHAODN//apt construct is shown in Figure S8. The sample was purified post-annealing using size-exclusion chromatography (SEC) with a flow rate of 0.5 mL/min and PBS as the mobile phase (Figure S9). The collected construct fractions were concentrated using centrifugal filters. Both SDS and native gel electrophoresis confirmed the efficient removal of free aptamer and residual rHAODN upon purification (Figure S10). A BCA protein assay was performed using a standard calibration with rHA to quantify the rHAODN//apt construct. The samples were stored at 4°C until further use. A concentration-dependent reduction in FIXa activity was observed at rHAODN//apt construct solutions of 1–100 nM (Figure 5). The result with the cODN-aptamer alone is shown in Figure S11. As a control, it was shown that rHAODN itself did not influence the FIXa assay in the presence of titrated amounts of rHAODN (Figure S12).

Human FcRn Affinity Studies

The ability of the rHAODN//apt construct to bind to human FcRn (hFcRn) was investigated with biolayer interferometry using immobilized hFcRn biosensors. Association and dissociation measurements were performed at pH 5.5 to reflect the endosomal environment needed to facilitate FcRn engagement,[16] and regeneration of the biosensor was performed at neutral pH 7.4 to reset the biosensor and remove any hFcRn-bound material. The binding affinities, K_D, were calculated based on a 1:1 binding model and the determined kinetic parameters k_{on} and k_{off} (Figure 6; Table 1). The assembled albumin-aptamer construct rHAODN//apt exhibited FcRn engagement; however, the affinity was reduced 9× compared to non-modified rHA (K_D 8.80 ± 2.17 μM and K_D 0.98 ± 0.25 μM, respectively). We, therefore, introduced a recombinant high-binding albumin variant (HB)[27] that has a higher hFcRn affinity (K_D 0.10 ± 0.008 μM) compared to wild-type rHA. Albumin-aptamer constructs prepared with the HB albumin (HBODN//apt) demonstrated 30× higher hFcRn affinity compared with wild-type rHAODN//apt (K_D 0.28 ± 0.08 μM; Figures 6 and S13; Table 1) and at least 3× higher affinity to hFcRn than the non-modified wild-type rHA alone.

Stability of the rHAODN//apt Conjugate in Serum-Containing Buffer

The rHAODN//apt construct and the FIXa aptamer were found to exhibit the same degree of stability when incubated in 10% serum for 12 and 24 hr at 37°C and analyzed by agarose gel electrophoresis (Figures 7A and 7B). Approximately 80% of the material was still intact after 24 hr in both cases (Figure 7C). Over the course of 24 hr, the cODN-modified aptamer alone appeared to be partially digested to a fragment migrating similarly to the naked FIXa aptamer (Figure S14A). This is most likely due to digestion of the cODN component when not engaged in the duplex of the rHAODN//apt

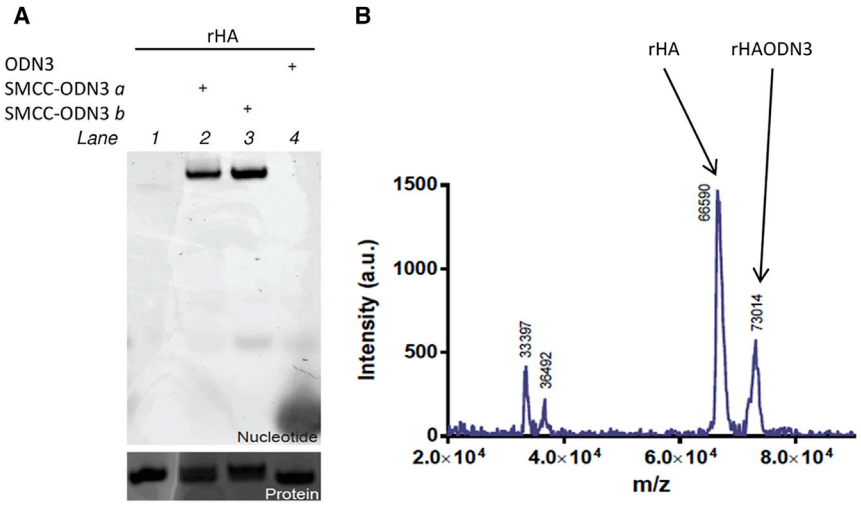

Figure 3. Conjugation of ODN to rHA

(A) SDS gel electrophoresis of ODN3 conjugated to rHA using maleimide chemistry. SYBR gold staining (upper panel) and Coomassie staining (lower panel) confirm conjugation to rHA of two different batches of ODN3 (SMCC-ODN3 *a* and SMCC-ODN3 *b*). (B) MALDI-ToF analysis of rHAODN3 conjugate showing the unmodified rHA at m/z = 66,590 and the conjugate rHAODN3 at m/z = 73,014 (calculated 73,360; MW(ODN3) = 6,550.4 g mol^{-1} and MW(SMCC-ODN3) = 6,770.0 g mol^{-1}). MW, molecular weight.

construct. rHA alone could not be visualized by SYBR GOLD staining (data not shown), and the faint band observed for the rHAODN conjugate most likely originates from the staining of the ODN strand (Figure S14B). This band also disappeared within 24 hr, suggesting that, as for the DNA strand of the cODN-aptamer, the DNA strand of rHAODN is also protected from digestion in the rHAODN//apt construct. Hence, the rHAODN//apt assembly is stable in serum-containing buffer.

DISCUSSION

Blood circulatory half-life extension technologies are required to extend the therapeutic effect of drugs susceptible to rapid renal clearance, such as RNAi- and aptamer-based molecular medicines. PEGylation is an established drug half-life extension technique; however, concerns regarding tissue accumulation of non-biodegradable high-molar mass PEG and complement activation have been raised.[9,11] HSA with a blood circulatory half-life of ~19 days therefore offers a biocompatible natural alternative.[10,14] The pronounced circulatory half-life of HSA is predominately facilitated by engagement of HSA with the cellular recycling FcRn.[16,17] Control over site-specific modification on HSA is thought to be a prerequisite in order to maintain FcRn engagement with DIII that is the principal binding site of HSA.[19] The single free cys34 in DI is distant to the main FcRn-engagement site in DIII and therefore offers an opportunity to conjugate drugs without compromising DIII interactions. This single site, however, only allows monofunctionalization. In this work, we present a cys34 site-specific albumin-dsDNA assembly approach to overcome this issue, allowing addition of functionalities to the three free oligo terminals.

Lau et al.[28] described siRNA-albumin conjugation using the 3′ end amine-modified siRNA, which was activated with a commercial NHS-maleimide linker (SMCC). The high specificity of the maleimide group toward thiols facilitated siRNA conjugation to the endogenous albumin pool, leading to a half-life extension from 5.1 ± 0.2 min to 75.9 ± 18.2 min in Sprague-Dawley rats.[29] For our approach, either 5′ or 3′ end amine-modified ODNs were modified with SMCC to allow attachment of ODN-cODN pairs to albumin in both orientations. Urea gel electrophoresis analysis and RP-HPLC analysis showed a pH and time-dependent trend for the efficiency of SMCC modification of ODNs, with maximum yields obtained using pH 8 and 16–24 hr of incubation. The SMCC activation was investigated for both 3′ and 5′ end amine-modified ODNs, ODNs of different sequences, and ODNs with or without a fluorophore in the opposite end, showing no obvious differences with respect to the efficiency of the reaction.

The free thiol of rHA at position 34 is prone to Michael-addition reactions on the maleimide-functional ODN.[29] The available thiol content of rHA was determined using an Ellman's assay prior to the conjugation of rHA with activated ODNs. Comparing the results from the Ellman's assay with the yields of ODN conjugation indicates a quantitative Michael-addition for both the 5′ and 3′ end activated ODNs. SMCC-unmodified ODN incubated with rHA showed no band shift by gel electrophoresis that indicated absence of non-covalent association of ODN with rHA. For rHAODN purification in our work, the large charge difference between residual rHA and rHAODN promotes IEX as a suitable method. Unfortunately, due to yet unknown reasons, after IEX and subsequent desalting, yields of purified rHAODN were approximately 10%, which requires improvements.

Annealing of rHAODN conjugates with cODN to form the rHAODN//cODN assembled constructs was investigated and confirmed with fluorophore-labeled ODN (direct labeling) as well as fluorophore-labeled cODN (indirect labeling). Hence, the assembly of rHAODN//cODN constructs appears to be compatible with loading of functionalities onto both the ODN and cODN, potentially allowing combinatorial applications.

FIXa plays an important role in blood coagulation and is a target for antithrombotic approaches. Currently available anticoagulants, however, can exhibit severe side effects, such as bleeding.[5] Rusconi et al.[4] described an aptamer-based FIXa inhibitor and an aptamer-blocking complementary oligonucleotide antidote allowing for controllable

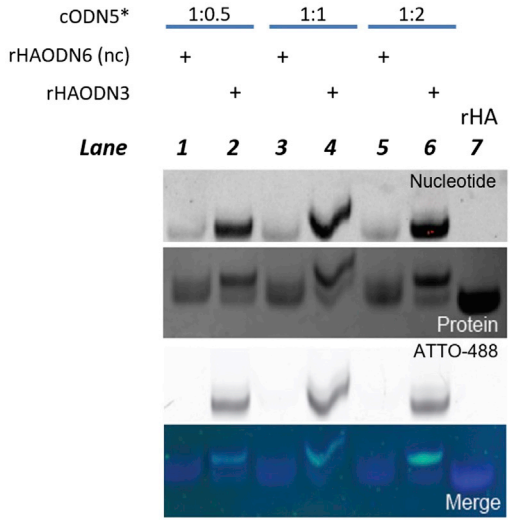

Figure 4. SDS Gel Electrophoresis Analysis of rHAODN3 and cODN5* Annealing

The gel was stained for ODN/cODN detection with SYBR gold (nucleotide) and for protein detection with Coomassie staining (protein). The labeled complementary strand cODN5* was detected by Atto488 fluorescence. The fluorophore detection and protein detection pictures were merged (merge). rHAODN6 and cODN5* annealing experiments were used as non-specific annealing negative control (nc) as ODN6 and cODN5* bear the same sequence. Annealing was performed with rHAODN3:cODN5* ratios of 1:0.5, 1:1, and 1:2. Free rHA was not separated from the rHAODN material before the analysis. The experiment represents one of three independent similar experiments.

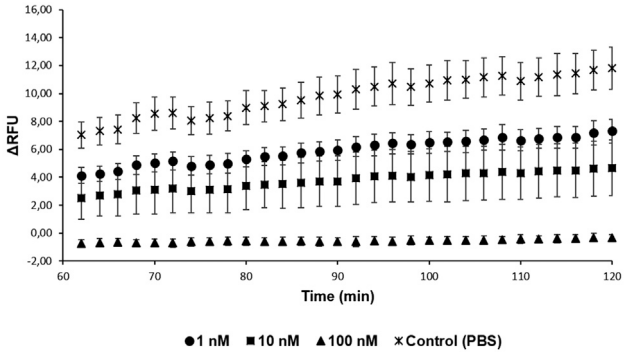

Figure 5. FIXa Activity Assay with rHAODN//apt

Substrate development (RFU) by FXa was monitored over time after incubation with FIXa. Preincubation of FIXa with increasing concentrations of the rHAODN//apt construct resulted in a lower activity of FXa (a reduced slope), indicating dose-dependent inhibitory activity toward FIXa-mediated conversion of FX to FXa. The figure shows the average and SDs of three experiments.

therapy. An increased aptamer blood circulation was shown by the same group using PEGylation.[30] The application of PEG as a half-life technology, however, may have drawbacks due to potential immunogenicity and tissue accumulation.[9,11] PEG immunogenicity was indeed suggested to be the reason for early termination of the recent phase 2b clinical trial with the FIXa aptamer antidote system (REG1).[12,13] In our work, the cODN-aptamer strand was designed so that the aptamer was positioned at the opposite site to rHA along the dsODN strand to reduce possible steric hindrance for annealing and aptamer target engagement. Experiments revealed that the cODN-aptamer strand could be successfully annealed to the rHAODN conjugate. rHAODN could not completely be removed by IEX, but elution time differences were sufficient in SEC for purification of the rHAODN//apt construct from any residual rHAODN. Aptamer activity after assembly with albumin was evaluated using a FIXa activity assay kit based on the cleavage of a substrate by FXa. FIXa activity measurements with the rHAODN//apt construct or the cODN aptamer showed that both blocked FIXa activity completely at a concentration of 100 nM, verifying that aptamer activity is retained following annealing.

Our conjugation design is based on attachment of ODN to rHA at a site distant from the region mainly responsible for FcRn engagement to ensure retained circulatory half-life extension exploitation. The rHAODN//apt construct exhibited FcRn engagement, although it was 9× lower compared to non-modified rHA. Some interference could be expected because aptamers are of considerable size compared to proteins.[31] Crystal structure[32] and interaction analysis studies[33] have, however, also revealed an hFcRn/albumin binding interface in the DI of albumin that is contributory toward optimal binding. In addition, recent work in our laboratory showed a decrease in albumin/hFcRn binding upon covalent attachment of mPEG at cys34.[34] To increase the FcRn affinity of the aptamer-albumin construct, a recombinant albumin variant engineered for high FcRn binding (referred to as HB albumin) was introduced. The HB albumin contains a single-point mutation in domain III, triggering a stronger FcRn interaction and concomitant extended half-life.[27] The HB shows 10x higher affinity toward hFcRn compared to rHA (Table 1) and hence is a useful tool to rescue the lost affinity introduced by the annealed aptamer. Although aptamer assembly with HB albumin (HBODN//apt) did reduce the hFcRn affinity of the HB albumin ∼3×, the affinity was improved 30× compared with rHAODN//apt and greater than rHA alone. Hence, the compromised albumin-FcRn interaction caused by aptamer albumin assembly could be re-established using the HB albumin variant. This is in accordance with recent studies from our laboratory showing that the reduction in hFcRn affinity after direct mPEG[34] and aptamer Cys34 conjugation[35] could be rescued by using the HB variant.

Finally, we showed that the assembled aptamer-albumin construct (including the dsDNA duplex) was stable in serum-containing buffer over 24 hr at 37°C to the same extent as the FIXa aptamer alone.

In this work, we present a novel albumin-ODN assembly method based on cys34-selective conjugation of ODNs and subsequent annealing of fluorophore- and aptamer-modified cODN strands. This versatile modular-based system offers potential blood circulatory half-life extension applications and combinations of drug and

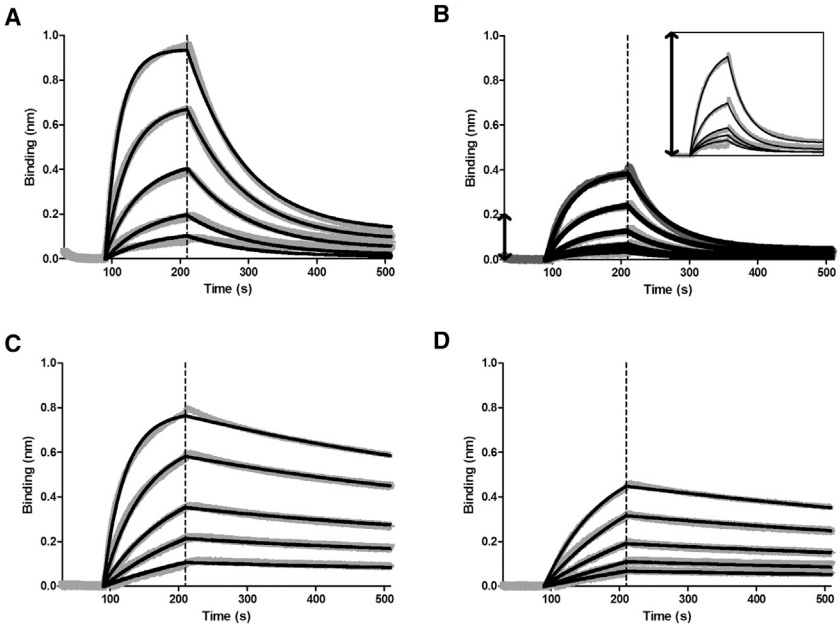

Figure 6. Representative hFcRn Binding Profiles
rHA (A), rHAODN//aptamer (B), HB (C), and HBODN//aptamer (D). Affinity assays were performed using a 2-fold dilution series from 3.0 to 0.1875 μM; however, for rHAODN//aptamer (B), an additional concentration of 6.0 μM was included to obtain a sufficient signal due to the weak hFcRn interaction. Raw data are depicted as gray binding curves and curve fittings overlaid as a darker thin line.

imaging types. The presented platform design shows the capability for three terminal functionalities; however, it also provides a framework design to expand the diversity and quantity by insertion of functionalized single nucleic acids or branching DNA structures as described by Horn et al.[36] or assemblies combining more than two strands.[37] The therapeutic aptamer constructs were stable in serum-containing buffer and retained FcRn engagement, prerequisites for potential in vivo applications.

MATERIALS AND METHODS

Materials

All ODNs with or without fluorophores were purchased from DNA Technology (Risskov, Denmark). ODNs were supplied as lyophilized pellets and resuspended in nuclease-free water at 1 mM prior to use. The concentration was validated by measuring A260 on a NanoDrop ND1000. rHA (Albucult) was obtained from Sigma-Aldrich (Copenhagen, Denmark). Recombinant HB albumin (K573P) was kindly provided by Albumedix (Nottingham, UK). SMCC was obtained from Sigma-Aldrich and dissolved in dry DMSO at 100 mM prior to use; aliquots were stored at −20°C. Protogel (30%) and UreaGel concentrate and UreaGel diluent were obtained by National Diagnostics (Atlanta, GA, USA). N,N,N',N'-tetramethylethylenediamine (TEMED), ammonium persulfate (APS), 5,5′-dithiobis-(2-nitrobenzoic acid) (DTNB) (Ellman's reagent), L-cysteine hydrochloride monohydrate, sodium phosphate dibasic hepta-hydrate, sodium phosphate monobasic monohydrate, Trizma base, Trizma hydrochloride, and EDTA were obtained from Sigma-Aldrich (Copenhagen, Denmark). APS was prepared as 10% stock solution in MilliQ. Gel cassettes and combs (Novex), NuPAGE, 2-(N-morpholino)ethanesulfonic acid (MES), and SDS Running Buffer (20×) (Novex) were obtained from Thermo Scientific (Slangerup, Denmark). SYBR Gold Nucleic Acid Gel Stain 10,000x was purchased from Invitrogen (Taastrup, Denmark). Protein assay dye reagent was obtained from Bio-Rad. FIXa activity assay (ab204727) was purchased from Abcam (Cambridge, UK).

Analytical and Preparative RP-HPLC

RP-HPLC was performed on an Agilent Technologies 1200 Series apparatus equipped with a C18 column (YMC-Pack Pro, 150 × 4.6 mm, AS-302-3, S-3 μm, 12 nm) to verify the SMCC activation of ODNs. A flow rate of 0.7 mL/min and UV detection at 260 nm were used. The product was eluted with A, triethylammonium acetate (TEAA) 0.05 M and 5% MeCN in H_2O; and B, MeCN using a gradient that was increased from 0% to 40% B over 15 min, followed by 40% to 100% B in 2 min, 2 min at 100% B, and 0% B in 3 min. Alternatively, a Kinetex C18 column and the following buffers were used: buffer A, 0.1 M TEAA with 10% acetonitrile filtered with a 0.2-μL filter; and buffer B, 100% acetonitrile. Samples were allowed to enter the column for 5 min with 100% buffer A, followed by an increase to 90% buffer B over 30 min at RT with a flow rate of 0.5 mL min^{-1}. Absorbance was measured at 260 nm as well.

Matrix-Assisted Laser Desorption/Ionization Time of Flight

Matrix-assisted laser desorption/ionization time-of-flight (MALDI-ToF) experiments were conducted on a Bruker Autoflex Speed. The used matrix was 15 mg mL^{-1} sinapic acid in a 1:1 mixture of Milli-Q water and acetonitrile. For spotting, each drop was allowed to dry before adding another drop. First, 2 × 1 μL matrix was spotted, then 1 μL sample solution (usually 4 μM), and finally 2 μL matrix on top.

IEX

IEX was performed using Pharmacia Biotech equipment. A Uvicors SII detector with a detection wavelength of 226 nm, a gradient pump 2249, a low pressure mixer, and a Degasys DG1310 degasser were used. Recording was performed with a Pharmacia Biotech LKB writer REC 2. The apparatus was equipped with an ion-exchange column (MonoQ, 50 × 5 mm, 10-μm particles) using a flow rate of 1 mL/min at RT. The product was eluted with A, 20 mM Tris-HCl and 10 mM NaCl, pH 7.6, and B, 20 mM Tris-HCl and 0.8 M NaCl, pH 7.6, using a gradient that was 0% B for 3 min, increased from 0% to 100% B in 27 min, and kept at 100% B for 3 min. B was reduced to 0% within 1 min afterward.

Table 1. Biolayer Interferometry hFcRn Affinity-Binding Studies of rHA, Annealed rHAODN//apt, hFcRn HB, and Annealed HBODN//apt

	K_D (μM)	$k_{on} \times 10^3$ ($1\ Ms^{-1}$)	$k_{off} \times 10^{-3}$ ($1\ s^{-1}$)
rHA	0.98 ± 0.25	11.2 ± 1.96	10.6 ± 0.64
rHAODN//apt	8.80 ± 2.17	1.73 ± 0.31	14.8 ± 1.00
HB	0.10 ± 0.008	10.8 ± 0.14	1.04 ± 0.10
HBODN//apt	0.28 ± 0.08	3.32 ± 0.31	0.95 ± 0.32

The K_D, k_{on}, and k_{off} values are averages of 3 measurements, each obtained using a 5-step dilution series from 0.1875 to 3.0 μM at pH 5.5, and for rHAODN//apt, a 6-step dilution from 0.1875 to 6.0 μM. All curves are fitted to a 1:1 binding model with the relation $K_D = k_{off}/k_{on}$.

SEC

SEC was performed using a Thermo Scientific Ultimate 3000 equipped with a fraction collector. Detection was performed at 224 nm using a UV-Vis detector. The apparatus was equipped with a size-exclusion column (Zenix SEC-300, 3 μm, 300 Å, 7.8 × 300 mm) using a flow rate of 0.5 mL/min at RT and PBS as solvent.

Urea-Poly(acrylamide) Gel Electrophoresis

Urea gel electrophoresis was used to investigate SMCC activation of ODN. For 30 mL, 15% polyacrylamide urea gel solution 18 mL UreaGel concentrate, 9 mL UreaGel diluent, and 3 mL 10x Tris-Borate-EDTA (TBE) buffer were mixed in a beaker by swirling. 100 μL APS (10%) was added and mixed, followed by 30 μL TEMED and mixing. Urea gel electrophoresis gels were run at 150 V for 1 hr and 45 min. Immediately after mixing the gel components, the solution was poured into gel cassettes and allowed to set for 30–60 min.

SDS-Poly(acrylamide) Gel Electrophoresis

SDS gel electrophoresis was performed using 10% gels made of Protogel. Conjugation and hybridization to ODN was evaluated using SDS gel electrophoresis. For 30 mL, 10% polyacrylamide SDS gel solution 10 mL ProtoGel, 8.1 mL 1.5 M Tris, pH 8.7, 200 μL 20% SDS, and 11.8 mL Milli-Q were mixed in a beaker by swirling. 225 μL 10% APS was added and mixed, and finally 20 μL TEMED was added and mixed. SDS gels were run at 150 V for 50 min. Immediately after mixing the gel components, the solution was poured into gel cassettes and allowed to set for 30–60 min. Gels were scanned using a Gel Doc EZ Imager (Bio-Rad) or a Typhoon Trio+ (GE Healthcare). Atto488 and SYBR Gold were detected using the 488/555 excitation/emission settings. Coomassie was detected by colorimetry or using 633/no bandpass excitation/emission settings. Gels were analyzed using Image Lab (Bio-Rad) or ImageJ software.

Native Gel Electrophoresis

Native gel electrophoresis was performed with an 8% gel. For this, 2.7 mL Protogel, 6.3 mL MilliQ, 1 mL 10x TBE buffer, 100 μL 10% APS, and 10 μL TEMED were mixed and poured into a gel cassette. A 12-well comb was inserted and the gel was crosslinked for 45 min. For loading, 2 μL solution and 2 μL loading buffer (1.5 mL glycerol in 10 mL MilliQ, stained with Orange G) were mixed and 4 μL were loaded into a well. The gel was run for 45 min at 150 V with TBE buffer as running buffer. The gel was directly used for SYBR gold staining or Coomassie staining. Gels were scanned using a Gel Doc EZ Imager (Bio-Rad) with the corresponding filter plate. Band analysis was performed using ImageJ.

Thiol Quantification (Ellman's Assay)

The experiment was performed in a 96-well plate. Samples were prepared in 100 μL volume in 0.1 M Tris-HCl, 0.01 M EDTA, pH 8.0, containing Trizma Base and Trizma HCl in Milli-Q water. rHA samples were analyzed in triplicates at a concentration of 62.5 μM. L-cysteine was prepared from 1 mM to 15.6 μM as calibration. After addition of a DTNB solution (0.01 M DTNB, 0.05 M sodium phosphate buffer, pH 7.0) and 15 min incubation, the absorbance at 412 nm was determined on a Biotek PowerWave XS2 spectrophotometer.

Protein Quantification (Bradford Assay)

The quantification was performed using a Bio-Rad protein assay dye reagent following the protocol of a microassay. Briefly, rHA solutions in nuclease-free water were prepared with a concentration range of 100–2.5 μg/mL. rHA calibration solutions (8 μL) were mixed with the pure dye concentrate (2 μL) as received. After 5 min incubation, a NanoDrop ND1000 was used to determine the absorbance at 595 nm using the Bradford assay method. The sensor was equipped with 2 μL solution and the absorbance was measured. This was performed in triplicate, and the absorbance values were fitted with a linear trendline, giving the calibration curve. The sample solutions were prepared with 2 μL dye and 8 μL sample solution as well, but using a dilution of 1:10 of the original sample to obtain data that fitted the calibration range.

Protein Quantification (BCA Protein Assay)

The quantification was performed using a Thermo Scientific Pierce BCA Protein Assay kit following the microplate procedure. Briefly, rHA solutions in nuclease-free water were prepared with a concentration range of 1,980–123.75 μg/mL. rHA calibration solutions (10 μL) were mixed with BCA working reagent (200 μL) in a 96-well plate. BCA working reagent was prepared from 50 parts BCA reagent A to 1 part BCA reagent B. The plate was covered and shaken for 60 s, followed by 60 min incubation at 37°C. After cooling to RT, a Varioskan LUX multimode microplate reader was used to determine absorbance at 562 nm. This was performed in triplicate, and the absorbance values were fitted with a non-linear least square fit giving the calibration curve. The sample solutions were prepared with 10 μL sample mixed with 200 μL working reagent.

Maleimide Functionalization of ODNs (Activation)

Amine-modified ODN and SMCC solutions were mixed as follows: 3 parts DMSO, 2 parts 1 mM ODN, 6 parts 0.1 M HEPES adjusted to pH 8.0, and 1 part 100 mM SMCC in DMSO. As an example, DMSO (15 μL) was mixed with ODN (ODN3 10 μL, 1 mM, 10 nmol) in an Eppendorf tube. HEPES buffer (30 μL, 0.1 M) was added and mixed well. Finally, SMCC (5 μL, 100 mM in DMSO,

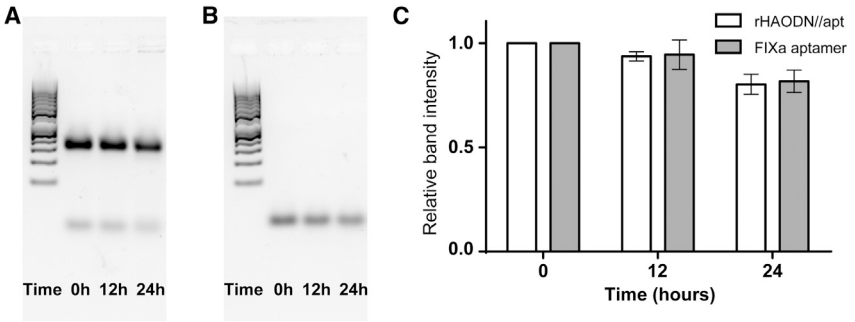

Figure 7. Stability of the Aptamer-Albumin Construct in 10% Serum

The aptamer-albumin construct rHAODN//apt (A) or FIXa aptamer (B) was incubated in 10% serum for 0, 12, and 24 hr at 37°C, and the degradation was analyzed by agarose gel electrophoresis. The DNA ladder contained 50, 100, 150, 200, 250, 300, 400, 500, 600, 700, 800, 900, and 1,000 bp products. (C) Band intensity for the rHAODN//apt construct and the FIXa aptamer at each time point was quantified, and the average of three independent experiments is shown relative to the 0 time point. Error bars show SD.

500 nmol) was added and a white precipitate appeared (NHS). The tube was closed and the mixture was shaken at 650 rpm overnight at RT. For purification, the mixture volume was increased to 200 μL with nuclease-free water and centrifuged using 14,000 × *g* for 10 min to collect the NHS precipitate. The supernatant was used for RP-HPLC analysis as well as for purification purposes using a fraction collector. The unreacted ODN eluted at 10.5 min and SMCC-activated ODN eluted at 11.5 min. Fractions were collected in 260-μL portions. The fractions with the activated ODN were collected and the material was allowed to dry out.

SMCC-ODN Conjugation to rHA

The quantity of activated SMCC-ODN was determined based on the initial quantity used for activation and product conversion determined by RP-HPLC. The dried SMCC-activated ODN was dissolved in nuclease-free H_2O to a concentration of 80 μM. As an example, activated ODN (conversion 50% by RP-HPLC, initial quantity 15 nmol equaling 7.5 nmol activated ODN, 1 equivalent [eq.]) was dissolved in 93.75 μL nuclease-free H_2O. rHA (10% solution [w/v], 20 μL, 30 nmol, 4 eq.) was added, and the mixture shaken at 650 rpm overnight at RT. The solution was purified from unreacted rHA using ion-exchange chromatography. The collected fractions were combined, and the salts were removed using a PD10 desalting column with nuclease-free water as the equilibration buffer. The eluted fractions were collected and the water was removed using a Christ RVC 2-18CDplus connected to a Christ Alpha 1-2 LDplus freeze dryer with pump.

Annealing of Complementary ODN to rHAODN Conjugates

The annealing was performed in annealing buffer (200 mM KOAc and 2 mM EDTA in nuclease-free H_2O). The conjugate solution (10 μL, 6.3 μM in nuclease-free H_2O, 63 pmol) was mixed with annealing buffer (20 μL) and heated in an Eppendorf tube to 55°C for 2 min. Concurrently, the complementary strand dissolved in nuclease-free water (10 μL, 6.3 μM in nuclease-free H_2O, 63 pmol) was heated for 2 min to 95°C and cooled down to 55°C. The complementary strand solution was transferred to the conjugate solution at 55°C and the heater was switched off and shaken in a thermoshaker with 650 rpm. After ~60 min, the solutions were at RT and shaken overnight. The solutions were directly analyzed using urea gel electrophoresis. Directly after gel electrophoresis, the gels were scanned for the Atto488 fluorophore using a Typhoon Trio+ scanner (GE Healthcare Life Sciences) with a blue laser (488 nm) and a 526-nm band-pass filter. Afterward, the gel was stained using standard Coomassie staining. After destaining, the gel was washed with TBE buffer three times to remove acetic acid and methanol from the gel. SYBR gold staining was performed according to the manufacturer's protocol. The Typhoon Trio+ scanner was used to scan for Coomassie staining without filter and excitation at 633 nm (red laser) as well as SYBR gold staining using a blue laser (488 nm) and a 555-nm band-pass filter.

Aptamer Production

The aptamer with (cODN-aptamer) or without a 3′ cODN extension (with a 5′-NH_2-C6 linker and a 3′- inverted deoxy-thymidine [idT]) was synthesized in a 1.0-μmol scale on a polystyrene dC support using the phosphoramidite approach and following the manufacturer's standard protocols. The coupling times for the commercially available 2′-deoxy-2′-fluoro-RNA, 2′-*O*-methyl-RNA, 2′-*O*-TBDMS-RNA, and DNA phosphoramidites were 12, 16, 12, and 10 min respectively, and stepwise coupling efficiencies in all cases were >98.0%, as determined by the absorbance of trityl cation at 495 nm after detritylation using DCA in toluene (2%, v/v). DCI was used as the activator, except for the RNA coupling, for which 1H-tetrazole was used as activator. Cleavage from the solid support and removal of nucleobase-protecting groups was performed using a solution of methyl amine in ethanol (33%, w/w) for 12 hr at RT. After evaporation to dryness, desilylation was performed using a 15:7:10 mixture of *N*-methyl-2-pyrrolidone, triethylamine, and $Et_3N \cdot 3HF$ for 12 hr at RT. The resulting oligonucleotides were purified by ion-exchange HPLC and desalted using a NAP-10 Sephadex column (GE Healthcare) according to the manufacturer's instructions. The composition of the aptamer was confirmed by Maldi-MS (observed mass 13,339.8; calculated 13,339.4), and the purity as >95% by analytical ion-exchange HPLC.

Annealing of Aptamer to rHAODN

rHAODN solution (109 μM, nuclease-free water, 30 μL, 3.27 nmol) was heated to 45°C. Aptamer solution (100 μM, nuclease-free water, 30 μL, 3 nmol) was heated to 90°C for 1 min. Annealing buffer (60 μL, 2x, 400 mM KOAc, and 4 mM EDTA, pH 7.6) was heated to 45°C. At 45°C, rHAODN solution, aptamer, and annealing buffer were mixed. The solution was stored in the 45°C warm heating block and the block

was turned off. After cooling down to RT, the solution was stored at 4°C overnight. The solution was subjected to SEC purification, and collected fractions were concentrated using Amicon Ultra 0.5 mL centrifugal filters with a Nominal Molecular Weight Limit of 3,000. 500 µL eluted fraction was loaded into the filter device and spun at 14,000 × *g* for 10 min, performed over several sittings. The concentrated samples were recovered from the spin filter by reverse spin at 1,000 × *g* for 2 min. For biolayer interferometry, samples were washed one time with 500 µL nuclease-free water prior to recovery. Concentrated samples were analyzed using SDS and native gel electrophoresis. Coomassie and SYBR gold staining was used to visualize the protein and nucleic acids, respectively.

FIXa Activity Assay

The protocol provided by Abcam for FIXa activity was slightly modified. Experiments were performed in triplicate. In a 96-well plate (transparent bottom, black), 10 µL of a FIXa enzyme standard (4 pg/µL enzyme standard in assay buffer) was placed in every well except the blank wells that were filled with 10 µL PBS. cODN-aptamer, rHAODN, and rHAODN//apt solutions were prepared in PBS (100 nM, 10 nM, and 1 nM). For each well, 10 µL of each solution was mixed with 78 µL of assay buffer. These 88-µL portions were mixed thoroughly with the prior pipetted FIXa enzyme in the wells. For untreated control, 10 µL PBS was mixed with 78 µL assay buffer and mixed with the enzyme-containing wells. The wells left for blank (no enzyme) were also mixed with this 10 µL PBS/78 µL assay buffer mix per each well. The 96-well plates were incubated at 37°C for 15 min to allow FIXa:aptamer binding. To each well, 10 µL Reaction Mix (2 µL Enzyme Mix I, 6 µL phospholipids, and 2 µL Enzyme Mix II) was added and incubated for 15 min at 37°C. After incubation, 2 µL FXa substrate-AMC was mixed in each well. At 37°C the fluorescence development (excitation/emission [ex/em] = 360/450 nm) was recorded in kinetic mode on a Varioskan LUX multimode microplate reader. The samples were scanned every 2 min for 120 min. For data processing, the average blanks were subtracted from the values obtained for the samples. Relative fluorescent units (RFU) were plotted against time. Linear region of the fluorescence development was used for data analysis. The slope of the RFU development shows the activity of the FIXa enzyme able to produce FXa that cleaves the chromogenic substrate.

hFcRn Binding Studies

A BLItz system (ForteBio, Pall Life Sciences, Menlo Park, CA, USA) was used with hFcRn-immobilized biosensors attached by streptavidin-biotin interactions. The streptavidin biosensors were hydrated in PBS supplemented with 0.01% Tween 20 (PBST) (pH 7.4) for a minimum of 10 min prior to coating. Biotinylated hFcRn (Immunitrack ApS) diluted in PBST (pH 7.4) to 3 µg mL^{-1} was used for coating and washed in PBST (pH 7.4). Albumin or aptamer albumin construct binding was measured using association buffer (25 mM sodium acetate, 25 mM NaH_2PO_4, and 150 mM NaCl in PBST, pH 5.5) with increasing sample concentrations (0.1875, 0.375, 0.75, 1.5, and 3.0 µM). The association step lasted for 120 s, and the dissociation step lasted for 300 s. Sensor regeneration was performed in PBST (pH 7.4) in between measurements. Background was subtracted for all binding curves using a reference run in pure association buffer. Analysis was performed using the BLItz Pro 1.2 software, and data were fitted to a 1:1 binding model.

Serum Stability Assays

10 pmol of FIXa aptamer, cODN-aptamer (apt), rHAODN, rHA, or rHAODN//apt was incubated in 10 µL of 20 mM HEPES (pH 7.4) containing 140 mM NaCl and 10% fetal calf serum (Sigma-Aldrich) for 0, 12, and 24 hr at 37°C. Samples were then analyzed by 1.5% agarose gel electrophoresis using 1xTBE as running buffer and SYBR Gold in the gel. The DNA ladder used was the Generuler 50-bp DNA ladder (Thermo Fisher Scientific). Gels were scanned using the Gel Doc EZ Imager, and quantification of gel band intensity was performed with ImageJ.

SUPPLEMENTAL INFORMATION

Supplemental Information includes fourteen figures and one table and can be found with this article online at https://doi.org/10.1016/j.omtn.2017.10.004.

AUTHOR CONTRIBUTIONS

K.A.H., D.S., and K.B. provided conception of the research. M.K., J.B.R.H., A.V., G.T., M.T.L., J.S.S., E.S.S., D.M.D., and K.B. conducted, analyzed, and interpreted the experiments. M.K., M.T.L., D.M.D., and K.A.H. designed the experiments. J.W. designed and synthesized the aptamers. M.K., D.M.D., and K.A.H. wrote, reviewed, and edited the final manuscript.

CONFLICTS OF INTEREST

The authors declare no competing financial interest.

ACKNOWLEDGMENTS

The authors would like to thank Hans Christian Høiberg for technical guidance on the RP-HPLC. This work was supported by Danish Innovation Fund grant 102-2014-3.

REFERENCES

1. Zhou, J., Bobbin, M.L., Burnett, J.C., and Rossi, J.J. (2012). Current progress of RNA aptamer-based therapeutics. Front. Genet. *3*, 234.
2. Castanotto, D., and Rossi, J.J. (2009). The promises and pitfalls of RNA-interference-based therapeutics. Nature *457*, 426–433.
3. Lares, M.R., Rossi, J.J., and Ouellet, D.L. (2010). RNAi and small interfering RNAs in human disease therapeutic applications. Trends Biotechnol. *28*, 570–579.
4. Rusconi, C.P., Scardino, E., Layzer, J., Pitoc, G.A., Ortel, T.L., Monroe, D., and Sullenger, B.A. (2002). RNA aptamers as reversible antagonists of coagulation factor IXa. Nature *419*, 90–94.
5. Howard, E.L., Becker, K.C.D., Rusconi, C.P., and Becker, R.C. (2007). Factor IXa inhibitors as novel anticoagulants. Arterioscler. Thromb. Vasc. Biol. *27*, 722–727.
6. Keefe, A.D., Pai, S., and Ellington, A. (2010). Aptamers as therapeutics. Nat. Rev. Drug Discov. *9*, 537–550.
7. Sun, H., Zhu, X., Lu, P.Y., Rosato, R.R., Tan, W., and Zu, Y. (2014). Oligonucleotide aptamers: new tools for targeted cancer therapy. Mol. Ther. Nucleic Acids *3*, e182.
8. Jepsen, J.S., Sørensen, M.D., and Wengel, J. (2004). Locked nucleic acid: a potent nucleic acid analog in therapeutics and biotechnology. Oligonucleotides *14*, 130–146.

9. Barz, M., Luxenhofer, R., Zentel, R., and Vicent, M.J. (2011). Overcoming the PEG-addiction: well-defined alternatives to PEG, from structure-property relationships to better defined therapeutics. Polym. Chem. *2*, 1900–1918.

10. Howard, K.A. (2015). Albumin: the next-generation delivery technology. Ther. Deliv. *6*, 265–268.

11. Yang, Q., and Lai, S.K. (2015). Anti-PEG immunity: emergence, characteristics, and unaddressed questions. Wiley Interdiscip. Rev. Nanomed. Nanobiotechnol. *7*, 655–677.

12. Povsic, T.J., Vavalle, J.P., Aberle, L.H., Kasprzak, J.D., Cohen, M.G., Mehran, R., Bode, C., Buller, C.E., Montalescot, G., Cornel, J.H., et al.; RADAR Investigators (2013). A phase 2, randomized, partially blinded, active-controlled study assessing the efficacy and safety of variable anticoagulation reversal using the REG1 system in patients with acute coronary syndromes: results of the RADAR trial. Eur. Heart J. *34*, 2481–2489.

13. Ganson, N.J., Povsic, T.J., Sullenger, B.A., Alexander, J.H., Zelenkofske, S.L., Sailstad, J.M., Rusconi, C.P., and Hershfield, M.S. (2016). Pre-existing anti-polyethylene glycol antibody linked to first-exposure allergic reactions to pegnivacogin, a PEGylated RNA aptamer. J. Allergy Clin. Immunol. *137*, 1610–1613.e7.

14. Sleep, D., Cameron, J., and Evans, L.R. (2013). Albumin as a versatile platform for drug half-life extension. Biochim. Biophys. Acta *1830*, 5526–5534.

15. Chaudhury, C., Mehnaz, S., Robinson, J.M., Hayton, W.L., Pearl, D.K., Roopenian, D.C., and Anderson, C.L. (2003). The major histocompatibility complex-related Fc receptor for IgG (FcRn) binds albumin and prolongs its lifespan. J. Exp. Med. *197*, 315–322.

16. Schmidt, E.G.W., Hvam, M.L., Antunes, F., Cameron, J., Viuff, D., Andersen, B., Kristensen, N.N., and Howard, K.A. (2017). Direct demonstration of a neonatal Fc receptor (FcRn)-driven endosomal sorting pathway for cellular recycling of albumin. J. Biol. Chem. *292*, 13312–13322.

17. Sleep, D. (2015). Albumin and its application in drug delivery. Expert Opin. Drug Deliv. *12*, 793–812.

18. Larsen, M.T., Kuhlmann, M., Hvam, M.L., and Howard, K.A. (2016). Albumin-based drug delivery: harnessing nature to cure disease. Mol. Cell. Ther. *4*, 3.

19. Andersen, J.T., Dalhus, B., Cameron, J., Daba, M.B., Plumridge, A., Evans, L., Brennan, S.O., Gunnarsen, K.S., Bjørås, M., Sleep, D., et al. (2012). Structure-based mutagenesis reveals the albumin-binding site of the neonatal Fc receptor. Nat. Commun. *3*, 610.

20. Caspersen, M.B., Kuhlmann, M., Nicholls, K., Saxton, M.J., Andersen, B., Bunting, K., Cameron, J., and Howard, K.A. (2017). Albumin-based drug delivery using cysteine 34 chemical conjugates - important considerations and requirements. Ther. Deliv. *8*, 511–519.

21. Kratz, F., Müller-Driver, R., Hofmann, I., Drevs, J., and Unger, C. (2000). A novel macromolecular prodrug concept exploiting endogenous serum albumin as a drug carrier for cancer chemotherapy. J. Med. Chem. *43*, 1253–1256.

22. Kratz, F. (2014). A clinical update of using albumin as a drug vehicle - a commentary. J. Control. Release *190*, 331–336.

23. Krieg, A.M. (2002). CpG motifs in bacterial DNA and their immune effects. Annu. Rev. Immunol. *20*, 709–760.

24. Shi, F., and Hoekstra, D. (2004). Effective intracellular delivery of oligonucleotides in order to make sense of antisense. J. Control. Release *97*, 189–209.

25. Andersen, E.S., Dong, M., Nielsen, M.M., Jahn, K., Subramani, R., Mamdouh, W., Golas, M.M., Sander, B., Stark, H., Oliveira, C.L., et al. (2009). Self-assembly of a nanoscale DNA box with a controllable lid. Nature *459*, 73–76.

26. Seeman, N.C. (2007). An overview of structural DNA nanotechnology. Mol. Biotechnol. *37*, 246–257.

27. Andersen, J.T., Dalhus, B., Viuff, D., Ravn, B.T., Gunnarsen, K.S., Plumridge, A., Bunting, K., Antunes, F., Williamson, R., Athwal, S., et al. (2014). Extending serum half-life of albumin by engineering neonatal Fc receptor (FcRn) binding. J. Biol. Chem. *289*, 13492–13502.

28. Lau, S., Graham, B., Boyd, B.J., Pouton, C.W., and White, P.J. (2011). Commercially supplied amine-modified siRNAs may require ultrafiltration prior to conjugation with amine-reactive compounds. J. Nucleic Acids *2011*, 154609.

29. Lau, S., Graham, B., Cao, N., Boyd, B.J., Pouton, C.W., and White, P.J. (2012). Enhanced extravasation, stability and in vivo cardiac gene silencing via in situ siRNA-albumin conjugation. Mol. Pharm. *9*, 71–80.

30. Rusconi, C.P., Roberts, J.D., Pitoc, G.A., Nimjee, S.M., White, R.R., Quick, G., Jr., Scardino, E., Fay, W.P., and Sullenger, B.A. (2004). Antidote-mediated control of an anticoagulant aptamer in vivo. Nat. Biotechnol. *22*, 1423–1428.

31. Dupont, D.M., Thuesen, C.K., Bøtkjær, K.A., Behrens, M.A., Dam, K., Sørensen, H.P., Pedersen, J.S., Ploug, M., Jensen, J.K., and Andreasen, P.A. (2015). Protein-binding RNA aptamers affect molecular interactions distantly from their binding sites. PLoS One *10*, e0119207.

32. Oganesyan, V., Damschroder, M.M., Cook, K.E., Li, Q., Gao, C., Wu, H., and Dall'Acqua, W.F. (2014). Structural insights into neonatal Fc receptor-based recycling mechanisms. J. Biol. Chem. *289*, 7812–7824.

33. Sand, K.M.K., Bern, M., Nilsen, J., Dalhus, B., Gunnarsen, K.S., Cameron, J., Grevys, A., Bunting, K., Sandlie, I., and Andersen, J.T. (2014). Interaction with both domain I and III of albumin is required for optimal pH-dependent binding to the neonatal Fc receptor (FcRn). J. Biol. Chem. *289*, 34583–34594.

34. Petersen, S.S., Kläning, E., Ebbesen, M.F., Andersen, B., Cameron, J., Sørensen, E.S., and Howard, K.A. (2016). Neonatal Fc receptor binding tolerance toward the covalent conjugation of payloads to cysteine 34 of human albumin variants. Mol. Pharm. *13*, 677–682.

35. Schmøkel, J., Voldum, A., Tsakiridou, G., Kuhlmann, M., Cameron, J., Sørensen, E.S., Wengel, J., and Howard, K.A. (2017). Site-selective conjugation of an anticoagulant aptamer to recombinant albumins and maintenance of neonatal Fc receptor binding. Nanotechnology *28*, 204004.

36. Horn, T., and Urdea, M.S. (1989). Forks and combs and DNA: the synthesis of branched oligodeoxyribonucleotides. Nucleic Acids Res. *17*, 6959–6967.

37. Seeman, N.C. (2003). DNA in a material world. Nature *421*, 427–431.